



York, C. B., and Frascino Müller de Almeida, S. (2017) On extension-shearing bending-twisting coupled laminates. *Composite Structures*, 164, pp. 10-22. (doi:[10.1016/j.compstruct.2016.12.041](https://doi.org/10.1016/j.compstruct.2016.12.041))

This is the author's final accepted version.

There may be differences between this version and the published version. You are advised to consult the publisher's version if you wish to cite from it.

<http://eprints.gla.ac.uk/132787/>

Deposited on: 14 December 2016

Accepted Manuscript

On Extension-Shearing Bending-Twisting Coupled Laminates

Christopher Bronn York, Sérgio Frascino Müller de Almeida

PII: S0263-8223(16)31547-1
DOI: <http://dx.doi.org/10.1016/j.compstruct.2016.12.041>
Reference: COST 8096

To appear in: *Composite Structures*

Received Date: 16 August 2016
Revised Date: 7 December 2016
Accepted Date: 9 December 2016



Please cite this article as: York, C.B., de Almeida, S.F.M., On Extension-Shearing Bending-Twisting Coupled Laminates, *Composite Structures* (2016), doi: <http://dx.doi.org/10.1016/j.compstruct.2016.12.041>

This is a PDF file of an unedited manuscript that has been accepted for publication. As a service to our customers we are providing this early version of the manuscript. The manuscript will undergo copyediting, typesetting, and review of the resulting proof before it is published in its final form. Please note that during the production process errors may be discovered which could affect the content, and all legal disclaimers that apply to the journal pertain.

On Extension-Shearing Bending-Twisting Coupled

Laminates

Christopher Bronn York^{*†} and Sérgio Frascino Müller de Almeida

Department of Mechatronics and Mechanical Systems Engineering, University of São Paulo, Av. Professor Mello Moraes, 2231, São Paulo, SP, 05508-030, Brazil.

Abstract

This article presents details of the development of a special class of laminate, possessing *Extension-Shearing Bending-Twisting* coupling, necessary for optimised passive-adaptive flexible wing-box structures. The possibility of achieving a measurable drag reduction in cruise flight, without the cost or reliability issues associated with active control mechanisms, is of significant interest for achieving increased fuel burn efficiency, and meeting associated emissions targets. The introduction of passive *Bending-Twisting* coupling at the wing-box level has been previously demonstrated through laminate level tailoring with *Extension-Shearing* coupling only, but the limited design space and the possibility for ply terminations (to produce tapered thickness) effectively rule out this special class of laminate for practical construction. The study is now broadened to consider laminates with *Extension-*

^{*}Permanent address: Aerospace Sciences, School of Engineering, University of Glasgow, University Avenue, G12 8QQ, Glasgow, Scotland.

[†]Corresponding author: Tel: +44 (0)141 3304345, E-mail address: Christopher.York@Glasgow.ac.uk

Shearing and *Bending-Twisting* coupling, beyond the less well-known un-balanced and symmetric design rule or indeed balanced and symmetric designs with off-axis alignment. Results reveal a vast laminate design space with *Extension-Shearing* coupling that can be maximised without the unfavourable strength characteristics associated with off-axis alignment. Results also reveal that shear buckling strength can be maximised through *Bending-Twisting* coupling when load reversal is not a design constraint.

Keywords

Extension-Shearing, Bending-Twisting coupling; Shear Buckling; Non-dimensional Stiffness Parameters; Lamination Parameters; Laminate Stacking Sequences.

Nomenclature

A, A_{ij} = extensional stiffness matrix and its elements

B, B_{ij} = coupling stiffness matrix and its elements

D, D_{ij} = bending stiffness matrix and its elements

$E_{1,2}$, G_{12} = in-plane Young's moduli and shear modulus

H = laminate thickness (= number of plies, $n \times$ ply thickness, t)

k_{xy} = non-dimensional buckling load factor in shear

M = vector of moment resultants (= $\{M_x, M_y, M_{xy}\}^T$)

N = vector of force resultants (= $\{N_x, N_y, N_{xy}\}^T$)

n = number of plies in laminate stacking sequence

Q_{ij} = reduced stiffness elements

- Q'_{ij} = transformed reduced stiffness elements
 t = ply thickness
 U_E, U_G = laminate invariants for equivalent isotropic properties, E_{Iso} and G_{Iso}
 U_Δ, U_ν = laminate invariants for orthotropic properties and Poisson ratio
 x, y, z = principal axes
 z_k = layer k interface distance from laminate mid-plane
 $\boldsymbol{\varepsilon}$ = vector of in-plane strains ($= \{\varepsilon_x, \varepsilon_y, \gamma_{xy}\}^T$)
 $\boldsymbol{\kappa}$ = vector of curvatures ($= \{\kappa_x, \kappa_y, \kappa_{xy}\}^T$)
 λ = buckling half-wave
 ν_{ij} = Poisson ratio
 θ_k = ply orientation for layer k
 ξ_Δ^A, ξ_ν^A = lamination parameters for orthotropic extensional stiffness
 $\xi_{\Delta c}^A, \xi_{\nu c}^A$ = lamination parameters for coupled extensional stiffness
 ξ_Δ^D, ξ_ν^D = lamination parameters for orthotropic bending stiffness
 $\xi_{\Delta c}^D, \xi_{\nu c}^D$ = lamination parameters for coupled bending stiffness
 ζ = bending stiffness parameter for laminate ($= n^3$)
 ζ_\pm = bending stiffness parameter for angle-ply sub-sequence
 ζ_+, ζ_- = bending stiffness parameter for positive/negative angle-ply sub-sequence
 $\zeta_\circ, \zeta_\bullet$ = bending stiffness parameter for cross-ply sub-sequences
 $+, -, \pm$ = angle plies, used in stacking sequence definition
 \circ, \bullet = cross-ply, used in stacking sequence definition

Matrix sub-scripts

- 0 = All elements zero
- F = All elements Finite
- I = Iotropic form
- S = Specially orthotropic or Simple form

1. Introduction

This article is one in a series, investigating unique forms of thermo-mechanically coupling behaviour for laminated composite materials. These are described collectively in an original article [1], identifying all 24 possible coupling interactions between *Extension*, *Shearing*, *Bending* and *Twisting*.

Here, attention is focussed on the identification of laminated composite materials possessing mechanical *Extension-Shearing* and *Bending-Twisting* coupling, in which the in-plane properties are decoupled from out-of-plane properties. It complements two previous articles on isolated mechanical *Extension-Shearing* coupling [2] and isolated mechanical *Bending-Twisting* coupling [3].

The motivation for this study is to explore the potential for maximising *Extension-Shearing* coupling, whilst minimising the detrimental effects of *Bending-Twisting* coupling. It was demonstrated that this can be achieved with standard ply orientations used in current industrial design practice, without using off-axis alignment of the principal material axis [4,5]. This approach is known to have a detrimental effect on material strength constraints that must be avoided. Note that whilst *Bending-Twisting*

coupling has detrimental effects on compression buckling strength [3], it does have the potential to increase shear buckling strength, as this article will demonstrate.

A complete list of *Extension-Shearing Bending-Twisting* coupled laminate is therefore developed, beyond the less well-known un-balanced and symmetric design rule [6]. The listings contain laminates with up to 21 plies; or 42 plies if the data is interpreted as the symmetric half of the laminate stacking sequence definition.

Laminate stacking sequence configurations are derived in symbolic form together with dimensionless parameters from which the extensional and bending stiffness terms are readily calculated; solutions are therefore independent of the fibre/matrix system and angle-ply orientation.

Unlike many previous studies in the literature, the results are applicable to, and indeed presented as laminate designs containing 0° , 90° , 45° and -45° ply orientations only, which is standard industrial design practice.

Expressions relating the dimensionless parameters to the well-known ply orientation dependent lamination parameters are also given, together with graphical representations of feasible domains for a range of ply number groupings, i.e., a set of laminate designs with a specific number of plies (n).

Quasi-Homogeneous laminates are also introduced as an important sub-set of *Extension-Shearing Bending-Twisting* coupled laminates, since such laminates have concomitant orthotropic properties, i.e., matching orthotropic stiffness in extension and bending. Quasi-Homogeneous designs permit ply percentage and buckling strength contours to be mapped onto the same lamination parameter design space, and thus serve

to demonstrate the effect on buckling strength of ignoring the presence of *Bending-Twisting* coupling.

New insights are provided into the relative shear buckling strength with respect to lamination parameters and lamination parameter design spaces, by way of an introduction to an accompanying article [7], which explores in detail the effect of *Bending-Twisting* coupling on compression and shear buckling strength, and is applicable to the data presented here, as well as to data for laminates with Bending-Twisting coupling only [3].

The remainder of this article is arranged as follows. Section 3 provides an overview of mechanical coupling behaviour before details of the derivation of definitive listings of *Extension-Shearing Bending-Twisting* coupled laminate configurations are presented, with up to 21 plies. Section 4 provides information on the extent of the feasible design space for *Extension-Shearing Bending-Twisting* coupled laminates, including the dominant forms of sub-sequence symmetries. *Extension-Shearing Bending-Twisting* coupled laminates arises from un-balanced and symmetric designs [6], but symmetry is shown here to be a sufficient rather than a necessary constraint. Expressions for ply orientation dependent lamination parameters are also given, together with graphical representations, which allow the available design space to be visually interrogated. The use of ply percentage mapping, as an approach to design for bending stiffness, is also discussed in the context of Quasi-Homogeneous laminates. Section 5 describes the association between ply percentages and shear buckling strength for simply supported plates, through a similar mapping procedure. Classical Garland curves are then presented in a form that permits an assessment of the bounds on the shear buckling

strength of *Extension-Shearing Bending-Twisting* coupled laminates across a range of aspect ratios. Finally, conclusions are drawn in Section 6.

2. Mechanical Coupling

Laminated composite materials are characterized in terms of their response to mechanical (and/or thermal) loading, which is associated with a description of the coupling behaviour, unique to this type of material. The coupling behaviour relevant to this study is presented in Table 1, together with the others in this series of related articles. All share the common feature that couplings between in-plane (i.e., extension or membrane) and out-of-plane (i.e., bending or flexure) responses, hence thermal warping distortions, are eliminated by virtue of the fact that $B_{ij} \neq 0$ in Eq. (1). However, these laminates possess coupling between in-plane shearing and extension is present when $A_{xs} = A_{ys} \neq 0$, and bending and twisting when $D_{xs} = D_{ys} \neq 0$.

$$\begin{aligned} \begin{Bmatrix} N_x \\ N_y \\ N_s \end{Bmatrix} &= \begin{bmatrix} A_{xx} & A_{xy} & A_{xs} \\ A_{xy} & A_{yy} & A_{ys} \\ A_{xs} & A_{ys} & A_{ss} \end{bmatrix} \begin{Bmatrix} \epsilon_x \\ \epsilon_y \\ \gamma_s \end{Bmatrix} + \begin{bmatrix} B_{xx} & B_{xy} & B_{xs} \\ B_{xy} & B_{yy} & B_{ys} \\ B_{xs} & B_{ys} & B_{ss} \end{bmatrix} \begin{Bmatrix} \kappa_x \\ \kappa_y \\ \kappa_s \end{Bmatrix} \\ \begin{Bmatrix} M_x \\ M_y \\ M_s \end{Bmatrix} &= \begin{bmatrix} B_{xx} & B_{xy} & B_{xs} \\ B_{xy} & B_{yy} & B_{ys} \\ B_{xs} & B_{ys} & B_{ss} \end{bmatrix} \begin{Bmatrix} \epsilon_x \\ \epsilon_y \\ \gamma_s \end{Bmatrix} + \begin{bmatrix} D_{xx} & D_{xy} & D_{xs} \\ D_{xy} & D_{yy} & D_{ys} \\ D_{xs} & D_{ys} & D_{ss} \end{bmatrix} \begin{Bmatrix} \kappa_x \\ \kappa_y \\ \kappa_s \end{Bmatrix} \end{aligned} \quad (1)$$

Whilst Eq. (1) describes the well-known **ABD** relation from classical laminate plate theory, it is more often expressed using compact notation:

$$\begin{Bmatrix} \mathbf{N} \\ \mathbf{M} \end{Bmatrix} = \begin{bmatrix} \mathbf{A} & \mathbf{B} \\ \mathbf{B} & \mathbf{D} \end{bmatrix} \begin{Bmatrix} \boldsymbol{\epsilon} \\ \boldsymbol{\kappa} \end{Bmatrix} \quad (2)$$

The coupling behaviour, which is dependent on the form of the elements in each of the extensional **[A]**, coupling **[B]** and bending **[D]** stiffness matrices, is now described by

an extended subscript notation, defined previously by the Engineering Sciences Data Unit, or ESDU [8] and subsequently augmented for the purposes of this series of articles. Hence, laminates with coupling between Extension and Shearing, and Bending and Twisting, are referred to by the designation $\mathbf{A}_F\mathbf{B}_0\mathbf{D}_F$, signifying that the elements of the extensional stiffness matrix $[\mathbf{A}]$ are finite, i.e.:

$$\begin{bmatrix} A_{xx} & A_{xy} & A_{xs} \\ A_{xy} & A_{yy} & A_{ys} \\ A_{xs} & A_{ys} & A_{ss} \end{bmatrix} \quad (3)$$

the coupling matrix $[\mathbf{B}]$ is null, whilst all elements of the bending stiffness matrix $[\mathbf{D}]$ are finite, i.e.:

$$\begin{bmatrix} D_{xx} & D_{xy} & D_{xs} \\ D_{xy} & D_{yy} & D_{ys} \\ D_{xs} & D_{ys} & D_{ss} \end{bmatrix} \quad (4)$$

where the elements of the stiffness matrices are derived from the well know relationships:

$$\begin{aligned} A_{ij} &= \sum Q_{ij}' (z_k - z_{k-1}) \\ B_{ij} &= \sum Q_{ij}' (z_k^2 - z_{k-1}^2) / 2 \\ D_{ij} &= \sum Q_{ij}' (z_k^3 - z_{k-1}^3) / 3 \end{aligned} \quad (5)$$

Note that the term *fully uncoupled orthotropic* laminate is synonymous with *specialy orthotropic* or *Simple* laminate. Such laminates possess none of the coupling characteristics described above and are represented by the designation $\mathbf{A}_S\mathbf{B}_0\mathbf{D}_S$, since the elements of the extensional and bending stiffness matrices are *Simple* or specially orthotropic in nature, e.g. the bending stiffness matrix $[\mathbf{D}]$ becomes:

$$\begin{bmatrix} D_{xx} & D_{xy} & 0 \\ D_{xy} & D_{yy} & 0 \\ 0 & 0 & D_{ss} \end{bmatrix} \quad (6)$$

Extensionally Isotropic laminates, with the designation $\mathbf{A}_I\mathbf{B}_0\mathbf{D}_S$ and Fully Isotropic laminates, with the designation $\mathbf{A}_I\mathbf{B}_0\mathbf{D}_I$, represent sub-sets of *Simple* laminates and are useful for benchmarking purposes. In the former case, the extensional stiffness matrix with designation \mathbf{A}_S is replaced with \mathbf{A}_I to indicate extensional isotropy, given that:

$$A_{xx} = A_{yy} \quad (7)$$

$$A_{ss} = (A_{xx} - A_{xy}) / 2 \quad (8)$$

In the latter case, the bending stiffness matrix with designation \mathbf{D}_S is replaced with \mathbf{D}_I to indicate bending isotropy, and hence full isotropy, given that, in addition to the Eqs (7) and (8):

$$D_{ij} = A_{ij}H^2 / 12 \quad (9)$$

where H is the laminate thickness.

Quasi-Homogeneous laminates possess concomitant stiffness properties, i.e., matching stiffness in extension and bending, as described by Eq. (9); these are presented elsewhere for *Simple* or uncoupled laminates [1].

This article presents therefore the definitive list of cross-ply and/or angle-ply stacking sequences for *Extension-Shearing Bending-Twisting* (or **E-S;B-T**) coupling, with the designation $\mathbf{A}_F\mathbf{B}_0\mathbf{D}_F$, together with the dimensionless stiffness parameters from which the elements of the extensional $[\mathbf{A}]$ and bending stiffness $[\mathbf{D}]$ matrices are readily calculated. These new stacking sequences complement the definitive list of Fully

Orthotropic (or *Simple*) laminates, with the designation $\mathbf{A}_S\mathbf{B}_0\mathbf{D}_S$, for up to 21 plies [9] together with *Extension-Shearing* (or $\underline{\mathbf{E-S}}$) coupling, with the designation $\mathbf{A}_F\mathbf{B}_0\mathbf{D}_S$ [2] and *Bending-Twisting* (or $\underline{\mathbf{B-T}}$) coupling, with designation $\mathbf{A}_S\mathbf{B}_0\mathbf{D}_F$ [3]. These related mechanical coupling designations are summarized in Table 1.

3. Derivation of stacking sequences

In the derivation of this list for (but not restricted to) standard angle-ply configurations, i.e., ± 45 , 0 and 90° , the general rule of symmetry is relaxed. Symmetric stacking sequences are ubiquitous in composite laminate design practice, for the simple reason that their use guarantees the laminate will remain flat, or warp free, after high temperature curing [10]. Non-symmetric laminates are commonly associated with, or often (incorrectly) used to describe [11], configurations that warp extensively after high temperature curing. However, non-symmetric stacking sequence configurations will be shown to provide the same thermo-mechanical properties as their symmetric counterpart, but are part of a much larger and generally unexplored design space. Unbalanced stacking sequences introduce *Extension-Shearing* coupling, which is eliminated only by using matching pairs of angle-ply layers [8].

For compatibility with previously published data [12], similar symbols have been adopted for defining all stacking sequences that follow. However, additional symbols and parameters are necessarily included to differentiate between cross plies (0° and 90°), given that symmetry about the laminate mid-plane is no longer assumed.

The resulting sequences are characterized by sub-sequence symmetry using a double prefix notation, the first character of which relates to the form of the angle-ply sub-sequence and the second character to the cross-ply sub-sequence. The double prefix

contains combinations of the following characters: *A* to indicate Anti-symmetric form; *N* for Non-symmetric; and *S* for Symmetric. Additionally, for cross-ply sub-sequences only, *C* is used to indicate Cross-symmetric form.

To avoid the trivial solution of a stacking sequence with cross plies only, all sequences have an angle-ply (+) on one outer surface of the laminate. As a result, the other surface ply may have an angle-ply of equal (+) or opposite (−) orientation or a cross ply (○ or ●), which may be either 0 or 90°.

Non-dimensional parameters are derived with each stacking sequence, which provide a compact data set allowing the extensional and bending stiffness properties to be readily calculated for any fibre/matrix system and angle-ply orientation.

3.1 Development of non-dimensional parameters

The development of non-dimensional parameters is demonstrated, by way of an example for a 16-ply symmetric laminate stacking sequence $[+/\circ/\bullet/+\bullet/+_2/\circ]_S$, in Table 2. The first two columns of Table 2 provide the ply number and orientation, respectively, whilst subsequent columns illustrate the summations, for each ply orientation, of $(z_k - z_{k-1})$, $(z_k^2 - z_{k-1}^2)$ and $(z_k^3 - z_{k-1}^3)$, relating to the **A**, **B** and **D** matrices, respectively. Here, the distance from the laminate mid-plane, z , is expressed in terms of ply thickness t ; assumed to be unit value.

The non-dimensional parameters arising from the tabular summations are as follows.

For the extension stiffness matrix [**A**]: the number of (0° = 90°) cross plies

$$n_o = n_{\bullet} = \sum_o^A = 4,$$

the number of negative angle plies

$$n_- = \sum_-^A = 0$$

the number of positive angle plies

$$n_+ = \sum_+^A = 8$$

Due to the balanced nature of this class of laminate, angle ply results may be conveniently combined to a single parameter

$$n_{\pm} = n_+ + n_-.$$

and the total number of plies, $n = n_+ + n_- + n_o + n_{\bullet}$.

The coupling stiffness matrix **[B]** summations confirm that $B_{ij} = 0$ for this laminate.

For the bending stiffness matrix **[D]**: the bending stiffness parameter for (0° and 90°) cross plies, representing the relative contribution to the overall bending stiffness of the laminate, is given by:

$$\zeta_o = \zeta_{\bullet} = 4 \sum_o^D = 4 \times 256 = 1024,$$

and the bending stiffness parameter for positive angle plies

$$\zeta_+ = 4 \sum_+^D = 4 \times 512 = 2048,$$

where a factor of 4 is introduced to facilitate a direct relationship between the non-dimensional parameters for extensional stiffness, i.e., the total number of plies, n , and the non-dimensional parameters for bending stiffness, i.e.,

$$n^3 = 16^3 = \zeta = \zeta_o + \zeta_{\bullet} + \zeta_- + \zeta_+ = 4096$$

Extension-Shearing Bending-Twisting coupled (A_SB₀D_F) laminates satisfy the following non-dimensional parameter criteria:

$$n_+ \neq n_- \quad (10)$$

$$\zeta_+ \neq \zeta_-$$

whilst $n_+ = n_-$ and $\zeta_+ = \zeta_-$ are the conditions giving rise to the *Simple* laminate classes.

3.2 Extensional and Bending stiffness relations

Inserting the non-dimension parameters into Eqs (5) for the extensional [A] and bending [D] stiffness matrices gives the following relations:

$$A_{ij} = [n_+ Q'_{ij+} + n_- Q'_{ij-} + n_o Q'_{ij0} + n_\bullet Q'_{ij\bullet}] t \quad (11)$$

$$D_{ij} = [\zeta_+ Q'_{ij+} + \zeta_- Q'_{ij-} + \zeta_o Q'_{ij0} + \zeta_\bullet Q'_{ij\bullet}] t^3 / 12 \quad (12)$$

Containing the usual transformed reduced stiffness terms in Eqs. (11) and (12) are given by:

$$\begin{aligned} Q'_{xx} &= Q_{11} \cos^4(\theta) + 2(Q_{12} + 2Q_{66}) \cos^2(\theta) \sin^2(\theta) + Q_{22} \sin^4(\theta) \\ Q'_{xy} &= Q'_{yx} = (Q_{11} + Q_{22} - 4Q_{66}) \cos^2(\theta) \sin^2(\theta) + Q_{12} (\cos^4(\theta) + \sin^4(\theta)) \\ Q'_{xs} &= Q'_{sx} = [(Q_{11} - Q_{12} - 2Q_{66}) \cos^2(\theta) + (Q_{12} - Q_{22} + 2Q_{66}) \sin^2(\theta)] \cos(\theta) \sin(\theta) \\ Q'_{yy} &= Q_{11} \sin^4(\theta) + 2(Q_{12} + 2Q_{66}) \cos^2(\theta) \sin^2(\theta) + Q_{22} \cos^4(\theta) \\ Q'_{ys} &= Q'_{sy} = [(Q_{11} - Q_{12} - 2Q_{66}) \sin^2(\theta) + (Q_{12} - Q_{22} + 2Q_{66}) \cos^2(\theta)] \cos(\theta) \sin(\theta) \\ Q'_{ss} &= (Q_{11} + Q_{22} - 2Q_{12} - 2Q_{66}) \cos^2(\theta) \sin^2(\theta) + Q_{66} (\cos^4(\theta) + \sin^4(\theta)) \end{aligned} \quad (13)$$

and the reduced stiffness terms by:

$$\begin{aligned} Q_{11} &= E_1 / (1 - \nu_{12} \nu_{21}) \\ Q_{12} &= \nu_{12} E_2 / (1 - \nu_{12} \nu_{21}) = \nu_{21} E_1 / (1 - \nu_{12} \nu_{21}) \\ Q_{22} &= E_2 / (1 - \nu_{12} \nu_{21}) \\ Q_{66} &= G_{12} \end{aligned} \quad (14)$$

For compactness of the data presented in the definitive listing of laminate stacking sequences that follow, for each ply number grouping, n , Eqs. (12) are re-cast as:

$$\begin{aligned} A_{ij} &= \left[n_{\pm} (n_{+} / n_{\pm}) Q'_{ij+} + n_{\pm} (1 - n_{+} / n_{\pm}) Q'_{ij-} + n_o Q'_{ij0} + (n - n_{\pm} - n_o) Q'_{ij\bullet} \right] t \\ D_{ij} &= \left[\zeta_{\pm} (\zeta_{+} / \zeta_{\pm}) Q'_{ij+} + \zeta_{\pm} (1 - \zeta_{+} / \zeta_{\pm}) Q'_{ij-} + \zeta_o Q'_{ij0} + (\zeta - \zeta_{\pm} - \zeta_o) Q'_{ij\bullet} \right] t^3 / 12 \end{aligned} \quad (15)$$

to account for missing parameters n_{\bullet} and ζ_{\bullet} , the fact that $n_{+} \neq n_{-}$ in un-balanced laminates and the inclusion of the ratio ζ_{+} / ζ_{\pm} , indicating the degree of *Bending-Twisting* coupling.

3.3 Lamination parameters relations

Lamination parameters facilitate the graphical inspection of feasible design space for *Extension-Shearing Bending-Twisting* coupled laminates, which are presented in Section 4. They also facilitate the formulation of a simple proof for the non-dimensional parameter criteria for this class of laminate, given in Eqs (10); this is provided in the electronic appendix. In the context of the non-dimensional parameters presented in the current article, the necessary lamination parameters are related through the following ply orientation dependent expressions:

$$\begin{aligned} \xi_{\Delta}^A &= \left[n_{\pm} (n_{+} / n_{\pm}) \cos(2\theta_{+}) + n_{\pm} (1 - n_{+} / n_{\pm}) \cos(2\theta_{-}) \right. \\ &\quad \left. + n_o \cos(2\theta_o) + (n - n_{\pm} - n_o) \cos(2\theta_{\bullet}) \right] / n \\ \xi_{V}^A &= \left[n_{\pm} (n_{+} / n_{\pm}) \cos(4\theta_{+}) + n_{\pm} (1 - n_{+} / n_{\pm}) \cos(4\theta_{-}) \right. \\ &\quad \left. + n_o \cos(4\theta_o) + (n - n_{\pm} - n_o) \cos(4\theta_{\bullet}) \right] / n \\ \xi_{\Delta c}^A &= \left[n_{\pm} (n_{+} / n_{\pm}) \sin(2\theta_{+}) + n_{\pm} (1 - n_{+} / n_{\pm}) \sin(2\theta_{-}) \right. \\ &\quad \left. + n_o \sin(2\theta_o) + (n - n_{\pm} - n_o) \sin(2\theta_{\bullet}) \right] / n \\ \xi_{Vc}^A &= \left[n_{\pm} (n_{+} / n_{\pm}) \sin(4\theta_{+}) + n_{\pm} (1 - n_{+} / n_{\pm}) \sin(4\theta_{-}) \right. \\ &\quad \left. + n_o \sin(4\theta_o) + (n - n_{\pm} - n_o) \sin(4\theta_{\bullet}) \right] / n \end{aligned} \quad (16)$$

relating to extensional stiffness, and

$$\begin{aligned}
 \xi_{\Delta}^D &= \left[\zeta_{\pm} (\zeta_{+} / \zeta_{\pm}) \cos(2\theta_{+}) + \zeta_{\pm} (1 - \zeta_{+} / \zeta_{\pm}) \cos(2\theta_{-}) \right. \\
 &\quad \left. + \zeta_0 \cos(2\theta_0) + (\zeta - \zeta_{\pm} - \zeta_0) \cos(2\theta_{\bullet}) \right] / n^3 \\
 \xi_v^D &= \left[\zeta_{\pm} (\zeta_{+} / \zeta_{\pm}) \cos(4\theta_{+}) + \zeta_{\pm} (1 - \zeta_{+} / \zeta_{\pm}) \cos(4\theta_{-}) \right. \\
 &\quad \left. + \zeta_0 \cos(4\theta_0) + (\zeta - \zeta_{\pm} - \zeta_0) \cos(4\theta_{\bullet}) \right] / n^3 \\
 \xi_{\Delta c}^D &= \left[\zeta_{\pm} (\zeta_{+} / \zeta_{\pm}) \sin(2\theta_{+}) + \zeta_{\pm} (1 - \zeta_{+} / \zeta_{\pm}) \sin(2\theta_{-}) \right. \\
 &\quad \left. + \zeta_0 \sin(2\theta_0) + (\zeta - \zeta_{\pm} - \zeta_0) \sin(2\theta_{\bullet}) \right] / n^3 \\
 \xi_{vc}^D &= \left[\zeta_{\pm} (\zeta_{+} / \zeta_{\pm}) \sin(4\theta_{+}) + \zeta_{\pm} (1 - \zeta_{+} / \zeta_{\pm}) \sin(4\theta_{-}) \right. \\
 &\quad \left. + \zeta_0 \sin(4\theta_0) + (\zeta - \zeta_{\pm} - \zeta_0) \sin(4\theta_{\bullet}) \right] / n^3
 \end{aligned} \tag{17}$$

relating to bending stiffness.

Elements of the *Extension-Shearing* coupled extensional stiffness matrix [**A**] are related to the lamination parameters [13] by:

$$[\mathbf{A}] = H \begin{bmatrix} U_E + \xi_{\Delta}^A U_{\Delta} + \xi_v^A U_v & U_E - 2U_G - \xi_v^A U_v & \xi_{\Delta c}^A U_{\Delta} / 2 + \xi_{vc}^A U_v \\ U_E - 2U_G - \xi_v^A U_v & U_E - \xi_{\Delta}^A U_{\Delta} + \xi_v^A U_v & \xi_{\Delta c}^A U_{\Delta} / 2 - \xi_{vc}^A U_v \\ \xi_{\Delta c}^A U_{\Delta} / 2 + \xi_{vc}^A U_v & \xi_{\Delta c}^A U_{\Delta} / 2 - \xi_{vc}^A U_v & U_G - \xi_v^A U_v \end{bmatrix} \tag{18}$$

and the fully populated bending stiffness matrix [**D**] by:

$$[\mathbf{D}] = \frac{H^3}{12} \begin{bmatrix} U_E + \xi_{\Delta}^D U_{\Delta} + \xi_v^D U_v & U_E - 2U_G - \xi_v^D U_v & \xi_{\Delta c}^D U_{\Delta} / 2 + \xi_{vc}^D U_v \\ U_E - 2U_G - \xi_v^D U_v & U_E - \xi_{\Delta}^D U_{\Delta} + \xi_v^D U_v & \xi_{\Delta c}^D U_{\Delta} / 2 - \xi_{vc}^D U_v \\ \xi_{\Delta c}^D U_{\Delta} / 2 + \xi_{vc}^D U_v & \xi_{\Delta c}^D U_{\Delta} / 2 - \xi_{vc}^D U_v & U_G - \xi_v^D U_v \end{bmatrix} \tag{19}$$

where the laminate invariants are given in terms of the reduced stiffnesses of Eqs (14)

by:

$$\begin{aligned}
U_E &= (3Q_{11} + 3Q_{22} + 2Q_{12} + 4Q_{66})/8 \\
U_G &= (Q_{11} + Q_{22} - 2Q_{12} + 4Q_{66})/8 \\
U_\Delta &= (Q_{11} - Q_{22})/2 \\
U_\nu &= (Q_{11} + Q_{22} - 2Q_{12} - 4Q_{66})/8
\end{aligned} \tag{20}$$

It should be pointed out that U_E and U_G are invariants in the sense that they do not vary with change of in-plane coordinates. U_E and U_G are associated with the equivalent isotropic properties of the layer:

$$\begin{aligned}
U_E &= E_{iso} / (1 - \nu_{iso}^2) \\
U_G &= G_{iso}
\end{aligned} \tag{21}$$

where, E_{iso} , G_{iso} , and ν_{iso} , are the isotropic properties of the material. U_Δ is associated with the orthotropy along axes 1 and 2 and U_ν affects the laminate Poisson ratio.

The above equations are identical to the original equations. Only the notation has been reformulated. The authors believe that this new notation is more intuitive, as it refers to the physical interpretation of the invariants and lamination parameters. Also, since there are only two material properties for an isotropic material, only two invariants (U_E and U_G) are used to describe the isotropic properties of the composite layer. The original definition of lamination parameters uses three invariants (U_1 , U_4 and U_5) that are linearly dependent.

3.4 Numerical Example

For IM7/8552 carbon-fiber/epoxy material with Young's moduli $E_1 = 161.0\text{GPa}$ and $E_2 = 11.38\text{GPa}$, shear modulus $G_{12} = 5.17\text{GPa}$ and Poisson ratio $\nu_{12} = 0.38$, lamina thickness $t = 0.1397\text{mm}$ the 16-ply symmetric laminate stacking sequence $[+/\circ/\bullet/+/ \bullet/+_2/\circ]_s$, for which the non-dimensional parameters were developed in

Section 3.1 and Table 2, where $\zeta_{\pm} = 2048$ and $\zeta_{+}/\zeta_{\pm} = 1.0$ or 100%. For standard fibre angles $\theta = \pm 45^{\circ}$, 0° and 90° in place of symbols \pm , \circ and \bullet , respectively, the transformed reduced stiffnesses are given in Table 5.

The A_{ij} and D_{ij} follow from Eqs (15):

$$A_{11} = [8 \times 50894 + 4 \times 162660 + (16 - 8 - 4) \times 0] \times 0.1397 = 154,198 \text{ N/mm}$$

$$D_{16} = [2048 \times 37791 + 1024 \times 0 + (4096 - 2048 - 1024) \times 0] \times 0.1397^3 / 12 = 17584 \text{ Nmm}$$

The final stiffness matrices for the laminate follow:

$$[\mathbf{A}] = \begin{bmatrix} 154198 & 50206 & 42235 \\ 50206 & 154198 & 42235 \\ 42235 & 42235 & 51996 \end{bmatrix} \text{ N/mm}$$

$$[\mathbf{D}] = \begin{bmatrix} 64199 & 20903 & 17584 \\ 20903 & 64199 & 17584 \\ 17584 & 17584 & 21648 \end{bmatrix} \text{ Nmm}$$

The form of these stiffness matrices has special significance since $A_{11} = A_{22}$ by inspection, and calculation reveals that $A_{66} = (A_{11} - A_{12})/2$, indicating that this laminate is extensionally isotropic, as defined in Eqs (7) and (8). However, $A_{16} = A_{16} \neq 0$, hence the laminate must be described as possessing *Extension-Shearing* coupling. The apparent extensional isotropy is in fact lost for any off-axis alignment between the material and structural axes. Further calculation reveals that $D_{ij} = A_{ij}H^2/12$, hence the properties are quasi-homogeneous, as defined in Eq. (9); a relationship which is unchanged by off-axis alignment.

The extensional $(\xi_{\Delta}^A, \xi_v^A, \xi_{\Delta c}^A)$ and bending $(\xi_{\Delta}^D, \xi_v^D, \xi_{\Delta c}^D)$ lamination parameters are calculated from Eqs. (16):

$$\xi_{\Delta}^A = [8 \cos(90^\circ) + 4 \cos(0^\circ) + 4 \cos(180^\circ)] / 16 = 0.00$$

$$\xi_v^A = [8 \cos(180^\circ) + 4 \cos(0^\circ) + 4 \cos(360^\circ)] / 16 = 0.00$$

$$\xi_{\Delta c}^A = [8 \sin(90^\circ) + 4 \sin(0^\circ) + 4 \sin(180^\circ)] / 16 = 0.50$$

The bending lamination parameters from Eqs. (17):

$$\xi_{\Delta}^D = [2048 \cos(90^\circ) + 1024 \cos(0^\circ) + 1024 \cos(180^\circ)] / 4096 = 0.00$$

$$\xi_v^D = [2048 \cos(180^\circ) + 1024 \cos(0^\circ) + 1024 \cos(360^\circ)] / 4096 = 0.00$$

$$\xi_{\Delta c}^D = [2048 \sin(90^\circ) + 1024 \sin(0^\circ) + 1024 \sin(180^\circ)] / 4096 = 0.50$$

$$\xi_{vc}^A = \xi_{vc}^D = 0 \text{ by virtue of the use of standard ply angles } 0^\circ, 90^\circ, \pm 45^\circ.$$

Hence this Quasi-Homogeneous laminate is defined by the extensional lamination

parameters $(\xi_{\Delta}^A, \xi_v^A, \xi_{\Delta c}^A) = (0, 0, 0.5)$ and bending lamination parameters

$$(\xi_{\Delta}^D, \xi_v^D, \xi_{\Delta c}^D) = (0, 0, 0.5).$$

4. Results and Discussion

Table 3 summarizes the definitive list of *Extension-Shearing*, *Bending-Twisting* coupled laminate configurations, arranged according to sub-sequence symmetry, and expressed as a percentage of the total for each ply number grouping.

Ply number groupings, $n = 3, 4, 5$ and 6 , contain only 3, 2, 13 and 11 symmetric (*SS*) solutions, respectively, and have therefore been omitted from Table 3. Details of sub-sequence symmetries for ply groupings for $n = 19$ ($\Sigma = 5,733,946$), 20 ($\Sigma = 2,584,228$) and 21 ($\Sigma = 5,372,297,583$) are also omitted, but contain 4.2% (239,263), 8.5% (218,385) and less than 0.1% (961,059) symmetric sequences, respectively.

These results demonstrate that a much larger design space exists for *Extension-Shearing*, *Bending-Twisting* coupled laminates compared to their *Extension-Shearing* coupling only [2] or *Bending-Twisting* coupling only [3] counterparts. They also demonstrate that the less common design rule for un-balanced, symmetric designs, dominate the design space only for laminates with up to 12 plies. Other forms of sub-sequence symmetries dominate in higher ply number groupings.

Common design rules [10] suggest that anti-symmetric laminate designs eliminate *Bending-Twisting* coupling, and although this was found to be the case for laminates with *Bending-Twisting* coupling only [3], anti-symmetric *Extension-Shearing*, *Bending-Twisting* coupled laminates have been identified. Anti-symmetric laminate designs are usually associated with laminates in which the coupling stiffness matrix [B] is non-zero [15], and are assumed to lead to thermal warping distortions, which is not the case for any of the designs presented in this article. This summary of results therefore demonstrates that employing design rules based on laminate symmetry can lead to a substantial part of the design space being overlooked.

Abridged listings of stacking sequences and non-dimensional parameters are given in Tables A2 – A10 of the electronic appendix, representing each distinct form of sub-sequence symmetry found. As adopted in listings for *Simple* or uncoupled laminates [9,12], the stacking sequence configurations with *Extension-Shearing* and *Bending-Twisting* coupling are ordered in terms of ascending numbers of plies, n , (or bending stiffness parameter, $\zeta = n^3$). Also, within each ply number grouping they are ordered by increasing *blend ratio*, defined as the ratio of the number of positive (n_+) plies to the total number of angle plies (n_{\pm}), indicating the degree of *Extension-Shearing* coupling. Laminates with the same blend ratio are in turn ordered by ascending value of the

bending stiffness parameter for the angle plies ($\zeta_{\pm} = \zeta_+ + \zeta_-$). This is a logic approach for design, given that compression buckling strength increases directly with increasing ζ_{\pm} . However, to account for the presence of *Bending-Twisting* coupled laminates, a ratio (ζ_+/ζ_{\pm}) of the bending stiffness parameters for angle plies is also introduced. Sequences are ordered in descending order of $|(\zeta_+/\zeta_{\pm}) - (\zeta_-/\zeta_{\pm})|$ to reflect the increasing compression buckling strength that these designs possess as they approach their uncoupled ($|(\zeta_+/\zeta_{\pm}) - (\zeta_-/\zeta_{\pm})| = 0$) counterparts, and finally by descending order of $|\zeta_0/(\zeta_0 + \zeta_{\bullet}) - \zeta_{\bullet}/(\zeta_0 + \zeta_{\bullet})|$, representing the relative difference in bending stiffness of cross-ply sub-sequences; this is introduced for laminates with matching ζ and $|(\zeta_+/\zeta_{\pm}) - (\zeta_-/\zeta_{\pm})|$, since compression buckling strength of infinitely long plates is maximised when $\zeta_0/(\zeta_0 + \zeta_{\bullet}) = \zeta_{\bullet}/(\zeta_0 + \zeta_{\bullet})$. The numbering of sequences within each sub-symmetric form, described in the previous section, may therefore be readily extended for laminates with higher ply number groupings, n .

The numbers of Quasi-Homogeneous ($\mathbf{A}_F\mathbf{B}_0\mathbf{D}_F$) laminates are introduced as an important laminate sub-set, possessing concomitant properties, i.e., matching stiffness in extension and bending, as defined by Eq. (9). These configurations are summarised in Table 4 and listed in full in the electronic annex; grouped according to sub-sequence symmetry, number of plies, n , and descending order of lamination parameters $\xi_{\Delta}^A = \xi_{\Delta}^D$, $\xi_v^A = \xi_v^D$ and $\xi_{\Delta c}^A = \xi_{\Delta c}^D$, respectively, noting that $\xi_{vc}^A = \xi_{vc}^D = 0$ for the standard fibre orientations assumed, i.e., $\pm 45^\circ$, 0° and 90° .

4.1 Design space interrogation

For optimum design, ply angle dependent lamination parameters are often preferred, since these allow the stiffness terms to be expressed as linear variables within convenient bounds ($-1.0 \leq \xi_i \leq 1.0$). However, the optimized lamination parameters must then be matched to a corresponding laminate configuration within the feasible region. This process is challenging, but is aided by graphical representation of the lamination parameter design spaces for each of the sub-sequence symmetries, identified in Table 3(a), together with the corresponding abridged stacking sequence listings in Tables A2 – A10 of the electronic appendix. These are 3-dimensional spaces for extensional stiffness, due to the presence of *Extension-Shearing* coupling, i.e., $\xi_{\Delta c}^A \neq 0$, as well as for bending stiffness, due to the presence of *Bending-Twisting* coupling, i.e., $\xi_{\Delta c}^D \neq 0$. Standard ply orientations ($\pm 45^\circ$, 0° and 90°) have been chosen specifically because they have most relevance to current design practice, and also avoid the complication of presenting 4-dimensional data, which would be the case for general angle-ply orientations, i.e., $\pm\theta \neq \pm 45^\circ$, hence $\xi_{vc}^A, \xi_{vc}^D \neq 0$. Note that the majority of the lamination parameter design spaces are presented in Figs A1 – A7 of the electronic appendix. What follows is a comparison of the two major sub-sequence symmetries.

Figure 1 illustrates the 3 dimensional point clouds representing (a)-(c) extensional and (d)-(f) bending stiffness for individual laminate configurations with Non-symmetric angle- and cross-ply sub-sequences (NN) and $7 \leq n \leq 18$, listed in abridged form in Table A6. From the total of 837,988 configurations, there are only 1,520 unique points on the lamination parameter design space for extensional stiffness, and 508,630 unique points for bending stiffness, where each point may represent multiple solutions. There

is a clear bias in the position of the lamination parameter point cloud towards the positive ξ_{vc}^D region of the design space as a result of the first (surface) ply being set to $+45^\circ$; the point cloud would be mirrored about the ξ_{vc}^D axis if the signs of the angle plies were switched.

Figure 2 presents the 3-dimensional lamination parameter design spaces for Symmetric angle- and cross-ply sub-sequences (SS), with $3 \leq n \leq 18$, listed in abridged form in Table A10. These represent the un-balanced and symmetric designs generally associated with this laminate class. The 151,078 configurations are contained within the 1,469 unique points on the lamination parameter design space for (a)-(c) extensional stiffness and the 145,515 unique points for (d)-(f) bending stiffness.

4.2 Interpretation of Lamination parameter design spaces

The results of Figs 1 – 2 (and Figs A1 – A7) can be interpreted in a number of ways for the purposes of laminate design. The annotated lamination parameter design space of Fig. 3(a) indicates that stacking sequences corresponding to the points $(-1, 1)$, $(0, -1)$ or $(1, 1)$, contain, respectively, 90° plies, $\pm 45^\circ$ plies or 0° plies only. It can therefore be readily appreciated that points lying along the edge of the triangular feasible region defined by the line drawn between $(\xi_{\Delta}^A, \xi_v^A) = (0, -1)$ and $(1, 1)$ correspond to laminates with 0 and $\pm 45^\circ$ plies only, whereas those along the line between $(0, -1)$ and $(-1, 1)$ consist of ± 45 and 90° plies only. The Isotropic laminate corresponds to $(\xi_{\Delta}^A, \xi_v^A, \xi_{\Delta c}^A) = (0, 0, 0)$.

Practical design rules are often based on ply percentages [14], which can be mapped onto the lamination parameter design space as illustrated on Fig. 3(a) to help with

interpretation of the results. These rules often restrict the design space to the central triangular region indicated by bold lines indicating a minimum of 10% for each of the cross plies, 0° and 90° ; other sources [10] suggest the extended region shown with broken lines indicating a minimum of 20% for each of the angle plies, 45° and -45° .

Ply percentages are only generally applicable to the design of in-plane properties. However, Fig. 3(b) presents lamination parameters corresponding to the results of Table 4, with $7 \leq n \leq 21$ plies, which are listed in full in the electronic annex. These Quasi-Homogenous laminates permit the mapping of ply percentages onto the lamination parameter design space for bending stiffness $(\xi_\Delta^D, \xi_v^D, \xi_{\Delta c}^D)$. This explains the rationale behind the axis labels of Fig. 3(a) and (b); the lamination parameters for extensional and bending stiffness are identical for Quasi-Homogenous laminates, i.e., $(\xi_\Delta^A, \xi_v^A, \xi_{\Delta c}^A) = (\xi_\Delta^D, \xi_v^D, \xi_{\Delta c}^D)$. There is no closed form buckling solution for shear buckling of infinitely long plates, hence buckling factor results, $k_{xy, \infty} (= N_{xy, \infty} b^2 / \pi^2 D_{Iso})$, were generated at each of the 15 equally spaced grid points across the lamination parameter design space of Fig. 3(b), using an exact infinite strip analysis [16], from which the following 4th order polynomial is then readily derived:

$$\begin{aligned}
 k_{xy, \infty} = & 5.336 - 2.914\xi_\Delta^D - 0.518\xi_v^D - 1.303(\xi_\Delta^D)^2 - 0.213(\xi_v^D)^2 + 1.048\xi_\Delta^D \xi_v^D \\
 & - 0.236(\xi_\Delta^D)^3 + 0.031(\xi_v^D)^3 - 0.197\xi_\Delta^D (\xi_v^D)^2 + 0.405(\xi_\Delta^D)^2 \xi_v^D - 0.443(\xi_\Delta^D)^4 \\
 & - 0.001(\xi_v^D)^4 + 0.022\xi_\Delta^D (\xi_v^D)^3 - 0.185(\xi_\Delta^D)^2 (\xi_v^D)^2 + 0.472(\xi_\Delta^D)^3 \xi_v^D
 \end{aligned} \quad (22)$$

The normalisation of the shear flow is with respect to D_{Iso} , which corresponds to the first of Eq. (19) with $(\xi_\Delta^D, \xi_v^D) = (0, 0)$, representing the Isotropic laminate, giving rise to the classical buckling factor result [17], $k_{xy, \infty} = 5.34$. This equation is used to

generate shear buckling contours for the infinitely long plate with simply supported edges, which are mapped onto the lamination parameter design space of Fig. 3(c). Note that the number of significant figures in the coefficients of Eq. (22) have been reduced, but are sufficient to maintain a buckling factor accurate to 2 decimal places.

The top corners of the triangular region, representing laminates with 90° and 0° degree plies only, have shear buckling factors $k_{xy,\infty} = 4.91$ and 1.31 , respectively, whereas the bottom corner, representing laminates with $\pm 45^\circ$ plies only, has buckling factor $k_{xy,\infty} = 5.61$. By ignoring the effect of *Bending-Twisting* coupling designers are effectively using this contour map, which is applicable only to fully uncoupled laminates, i.e., $\xi_{\Delta c}^D$ (and ξ_{vc}^D) = 0.

The mapping of ply percentages to buckling factor contours for *Bending-Twisting* coupled laminates is possible because of concomitant *Extension-Shearing* coupling in Quasi-Homogeneous laminates.

The Quasi-Homogenous laminates illustrated in Figure 4 are an important sub-group, which permit the effect of increasing (*Extension-Shearing*) *Bending-Twisting* coupling magnitude, or $\xi_{\Delta c}^D$, to be studied, with orthotropic properties from across the design space of Figure 4(b). Complete laminate listings are therefore provided in Table A11 of the electronic appendix. They are listed in order of increasing ply number grouping and then by increasing order of lamination parameters $\xi_{\Delta}^A = \xi_{\Delta}^D$, $\xi_{\nu}^A = \xi_{\nu}^D$ and $\xi_{\Delta c}^D$, respectively; sequences approaching $\xi_{\Delta}^D = 0$, $\xi_{\nu}^D = -1$ and $\xi_{\Delta c}^D \approx 0.00$, possess the highest compression buckling factor, $k_{x,\infty} = N_{x,\infty} b^2 / \pi^2 D_{\text{Iso}}$ [3].

5. Effect of Bending-Twisting coupling on shear buckling load factor

Ignoring the effects of *Bending-Twisting* coupling continues to be broadly justified on the basis that the effects dissipate for laminates with a large number of plies. However, buckling strength is strongly influenced by such coupling in thin laminates; shear buckling strength may be overestimated (unsafe) or underestimated (over-designed) if the effects of *Bending-Twisting* coupling are ignored. This can be appreciated by the fact that shear loading and *Bending-Twisting* coupling ($\xi_{11} > 0$) both give rise to skewed nodal lines in the buckling mode shapes. Hence, the presence of *Bending-Twisting* coupling may augment or counter the effect of shear load depending on whether the resulting diagonal tension is perpendicular or parallel to the dominant angle-ply direction.

Note that the results presented in this section represent continuous plates, supported at regular plate length intervals, a , and whilst compression buckling results for isotropic plates are the same as those for isolated plates with simply supported edges, mode interaction, due to shear buckling, results in an increase in buckling strength compared to the isolated plate.

5.1 Details of analysis and modelling

The buckling results presented represent continuous or infinitely long plates and are obtained using the panel buckling analysis and optimum design code VICONOPT [16], which is based on the stiffness matrix method with exact flat plate theory; it can be described as an exact infinite strip theory.

VICONOPT is based on the earlier programs VIPASA and VICON. VIPASA (Vibration and Instability of Plate Assemblies with Shear and Anisotropy) theory

assumes that the mode of buckling varies sinusoidally in the longitudinal direction with half-wavelength, λ . This type of analysis was used only to generate the asymptotic values for Fig. 5, representing the infinitely long plate. VICON (VIPASA with CONstraints) theory uses Lagrangian multipliers to impose point constraints, so that rectangular boundaries can be accurately represented when the composite material possesses *Bending-Twisting* coupling or when the plate is loaded in shear; skewed nodal lines result in these cases. The analysis assumes that the deflections of the plate assembly can be expressed as a Fourier series, in which suitable combinations of half wavelengths are now coupled, in order to satisfy the point constraints. Thus results are for an infinitely long plate assembly, with supports repeating at panel length intervals, a .

5.2 Garland Curves

Lamination parameters are used in the labelling of the Garland curves for shear buckling factor, $k_{xy,\infty} (= N_{xy,\infty} b^2 / \pi^2 D_{\text{iso}})$, presented across a range of aspect ratios (a/b) in Fig. 5. The lamination parameter $-0.5 \leq \xi_{\Delta c}^D \leq 0.5$ is a measure of the magnitude of *Bending-Twisting* coupling for Quasi-homogeneous laminates in Fig. 5(a), chosen for their matching orthotropic lamination parameters $(\xi_{\Delta}^A, \xi_{\nu}^A) = (0, 0)$ and $(\xi_{\Delta}^D, \xi_{\nu}^D) = (0, 0)$; the bounds vary with $\xi_{\nu}^D (= \xi_{\nu}^A)$ up to a maximum of $-1 \leq \xi_{\Delta c}^D \leq 1$ when $\xi_{\nu}^D = -1$, which correspond to the Angle-ply laminate designs in Fig. 5(b); also chosen for their matching orthotropic lamination parameters $(\xi_{\Delta}^A, \xi_{\nu}^A) = (0, -1)$ and $(\xi_{\Delta}^D, \xi_{\nu}^D) = (0, -1)$.

In Fig. 5(a), comparisons are made between an equivalent fully uncoupled isotropic ($\mathbf{A}_I\mathbf{B}_0\mathbf{D}_I$) laminate datum and Quasi-Homogeneous *Extension-Shearing, Bending-Twisting* coupled ($\mathbf{A}_F\mathbf{B}_0\mathbf{D}_F$) laminate derived in Sections 3.1 and 3.4, where all elements of the \mathbf{ABD} matrix are identical except for $D_{16} (= A_{16} \times H^2/12) = D_{26} (= A_{26} \times H^2/12)$, which are zero in the $\mathbf{A}_I\mathbf{B}_0\mathbf{D}_I$ laminate. This comparison serves to isolate the effects of (*Extension-Shearing*) *Bending-Twisting* coupling for buckling strength comparisons.

The material properties used in the modelling of the equivalent Isotropic ($\mathbf{A}_I\mathbf{B}_0\mathbf{D}_I$) laminate datum configuration were consistent with those used in the numerical example of Sections 3.4, leading to: leading to: $E_{iso} = E_1 = E_2 = 61.7$ GPa, $\nu_{iso} = 0.326$ and $G_{iso} = 23.3$ GPa, from which $D_{iso} = E_{iso}H^3/(1 - \nu_{iso}^2)$ follows.

The asymptotes on Fig. 5(a) represent $k_{xy,\infty}$ for the infinitely long plate with edges simply supported, and reveal bounds on buckling strength increase (reduction), due to the presence of *Bending-Twisting* coupling, of up to 37% (34%) with respect to the fully Isotropic laminate, i.e., $\xi_{\Delta}^D = \xi_v^D = \xi_{\Delta c}^D = 0$, giving the classical buckling result, $k_{xy,\infty} = 5.34$. Note that this increase/reduction is realised in a practical design, e.g. the 16 ply laminate: $[+/\text{O}/\bullet/-/\bullet/+_2/\text{O}]_S$ with $\xi_{\Delta}^D = \xi_v^D = 0$ and $\xi_{\Delta c}^D = 0.5$, which sits on the boundary of the design space. The positive shear load and positive fibre orientation, which is associated with positive $\xi_{\Delta c}^D$, are defined in the thumbnail sketch on Fig. 5(a).

Reversing the shear load direction has the same effect as changing the sign of $\xi_{\Delta c}^D$, hence care must be exercised in laminate design if the possibility of load reversal exists.

Shear buckling results for Quasi-Homogeneous Angle-ply laminates with simple supports are presented on Fig. 5(b). Here, the asymptotes representing $k_{xy,\infty}$ reveal

bounds on buckling strength increase (reduction) of up to 58% (75%) with respect to Angle-ply laminates with $\xi_{\Delta}^D = \xi_{\Delta c}^D = 0$ and $\xi_v^D = -1$, e.g. the fully uncoupled anti-symmetric 16 ply laminate $[+/-/-/+/-/+/-/-]_A$. Bounds on shear buckling strength for practical designs also come close to these theoretical maxima. It should be noted that the definition of a practical design is open to question. The 10% rule is commonly adopted in design practice, representing the minimum fibre content requirement in each of the four principal directions (0° , 90° , 45° and -45°), and also a maximum ply contiguity constraint is often applied, i.e., the maximum number of adjacent plies with the same fibre orientation.

6. Conclusions

The definitive list of laminate stacking sequences for *Extension-Shearing*, *Bending-Twisting* coupling has been developed for up to 21 plies for lamination angles 0° , 90° , θ and $-\theta$, where $\theta = 45^\circ$ has been assumed in all the results presented. It has been shown to contain many forms of non-symmetric angle-ply and cross-ply sub-sequences, yet all configurations can be manufactured flat under a standard elevated temperature curing process by virtue of the decoupled nature between in-plane and out-of-plane behaviour.

The less common ‘un-balanced and symmetric’ design rule, normally assumed necessary to achieve this warp free condition, accounts for less than 0.03% of the design space within this range of ply number groupings investigated.

The definitive list has also been shown to contain Quasi-Homogeneous laminates, with concomitant stiffness properties between extensional and bending stiffness, which allow ply percentages for *Extension-Shearing* coupling to be directly related to the buckling strength effects due to *Bending-Twisting* coupling.

Comparisons of the shear buckling response of infinitely long plates with simply supported edges reveal that *Bending-Twisting* coupling results in buckling strength increase (reduction) of up to 37% (34%) with respect to the fully Isotropic laminate and up to 58% (75%) with respect to Quasi-Homogeneous Angle-ply laminates.

Acknowledgements

The Newton Research Collaboration Programme (NRCP1516/4/50) and Conselho Nacional de Desenvolvimento Científico e Tecnológico (CNPq 309545/2015-3 and 574004/2008-4) are gratefully acknowledged for supporting this research.

References

1. York, C. B. Unified approach to the characterization of coupled composite laminates: benchmark configurations and special cases. *Journal of Aerospace Engineering* 2010;23:219-242.
2. York, C. B. On Extension-Shearing coupled laminates. *Composite Structures*, 2015;120:472-482.
3. York, C. B. On Bending-Twisting coupled laminates. *Composite Structures*, (doi:10.1016/j.compstruct.2016.10.063).
4. Nixon, M.W. Extension-twist coupling of composite circular tubes with application to tilt rotor blade design. *Proceedings of the 28th AIAA/ASME/ASCE/AHS/ASC Structures, Structural Dynamics, and Materials*, Monterey, CA, USA, 1987.
5. Fukunaga, H. and Sekine, H. A laminate design for elastic properties of symmetric laminates with extension-shear and bending-twisting coupling. *Journal of Composite Materials*, 1994;28;708-731.

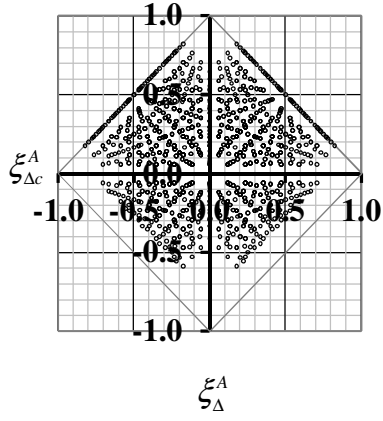
6. Baker, D. Response of Damaged and Undamaged Tailored Extension-Shear-Coupled Composite Panels. *J. Aircraft* 2006;43:517-527.
7. York, C. B. and Almeida, S. F. M. Effect of bending-twisting coupling on the compression and shear buckling strength of infinitely long plates. *Composite Structures*, Submitted for possible publication.
8. Engineering Sciences Data Unit. Stiffnesses of laminated plates. ESDU Item No. 94003, IHS, 1994.
9. York, C. B. Characterization of non-symmetric forms of fully orthotropic laminates. *J. Aircraft* 2009;46:1114-1125.
10. Niu, M. C. *Composite Airframe Structures*, 3rd Edition. Conmil Press, Hong Kong. 2000.
11. Jones, R. M. *Mechanics of Composite Materials*. Taylor & Francis, London, 1999.
12. Engineering Sciences Data Unit. Laminate stacking sequences for special orthotropy (Application to fibre reinforced composites). ESDU Item No. 82013, IHS, 1982.
13. Tsai, S.W., Hahn, H.T. *Introduction to composite materials*. Technomic Publishing Co. Inc., Lancaster, 1980.
14. Bailie, J. A., Ley, R. P. and Pasricha, A. A summary and review of composite laminate design guidelines. Task 22, NASA Contract NAS1-19347, 1997.
15. Li, D., and York, C. B. Bounds on the natural frequencies of laminated rectangular plates with extension-twisting (and shearing-bending) coupling. *Composite Structures*. 2015;131:37-46.

16. Williams, F. W. Kennedy, D. Butler, R. and Anderson, M. S. VICONOPT: Program for exact vibration and buckling analysis or design of prismatic plate assemblies. AIAA J. 1991;29:1927-1928.

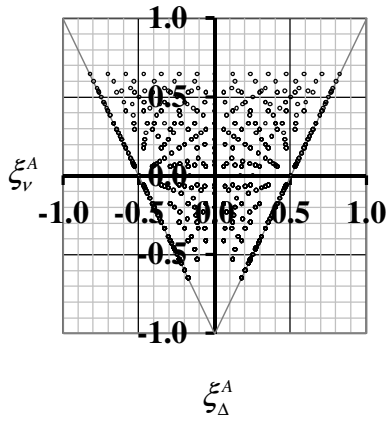
17. Southwell, R. V. and Skan, S. W. On the stability under shear forces of a flat elastic strip, Proceedings of the Royal Society of London, 1924; A105:582-607.

ACCEPTED MANUSCRIPT

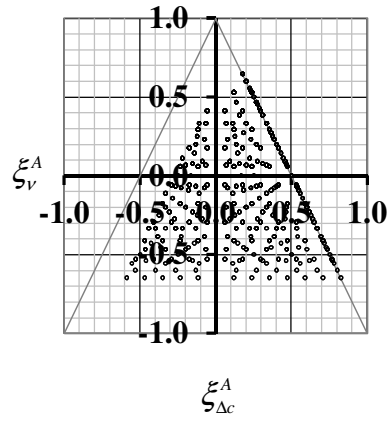
Figures



(a)

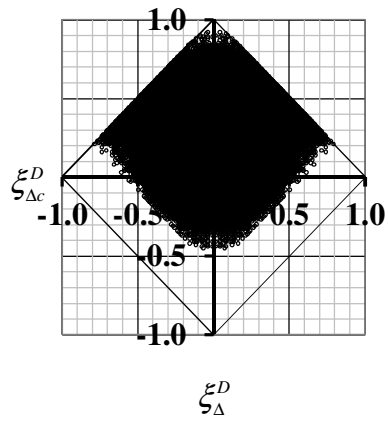


(b)

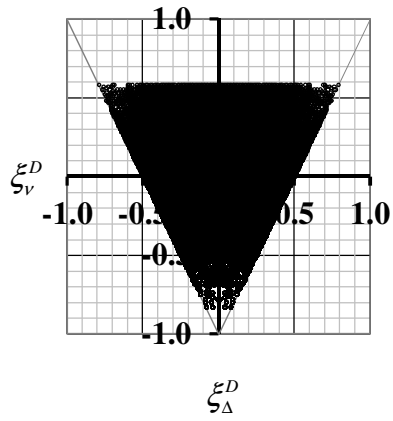


(c)

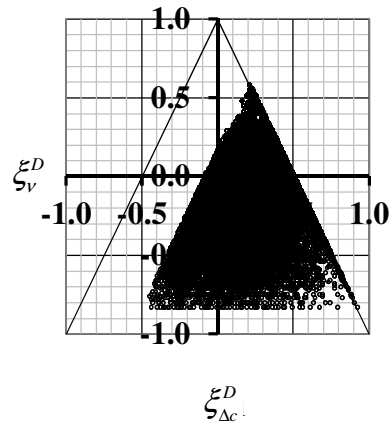
Figure 1



(d)

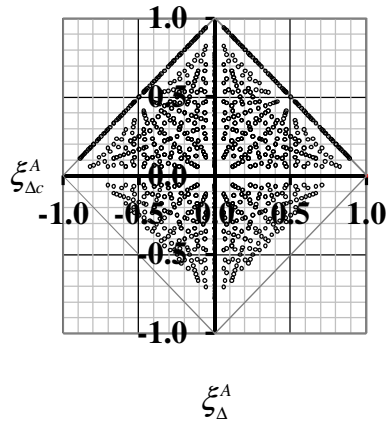


(e)

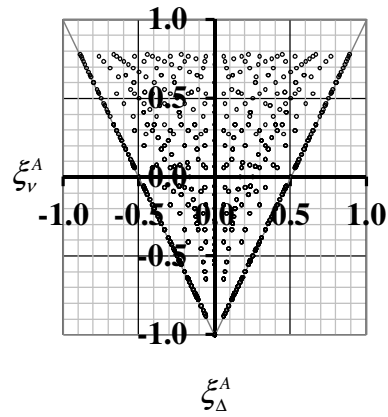


(f)

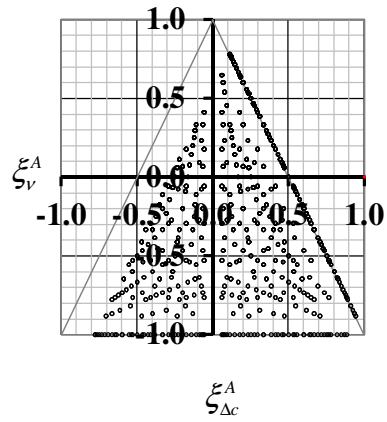
Figure 1



(a)

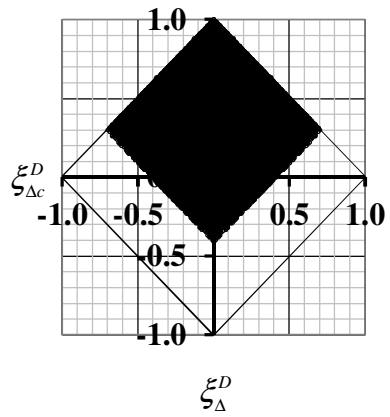


(b)

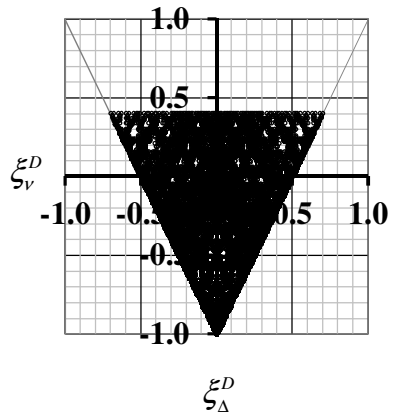


(c)

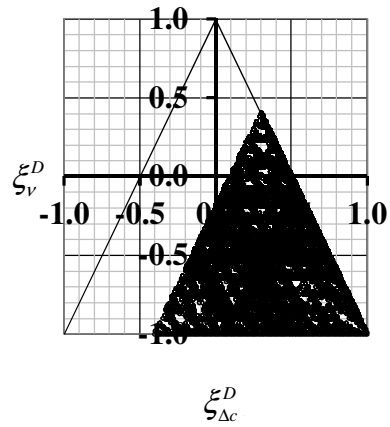
Figure 2



(d)

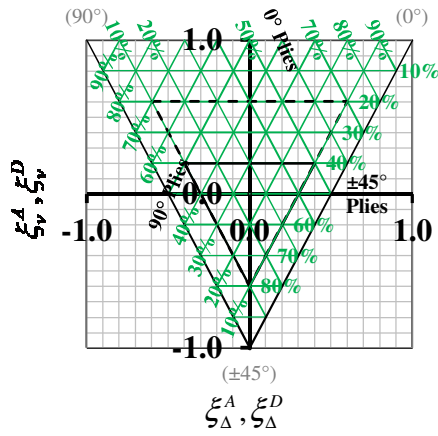


(e)

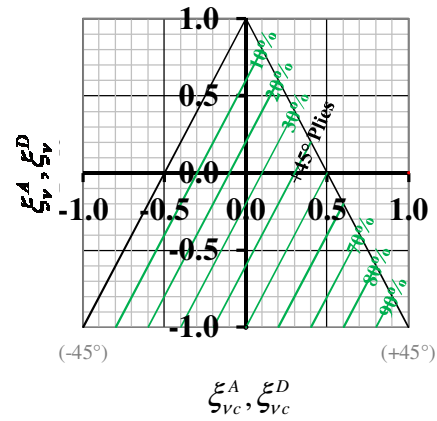


(f)

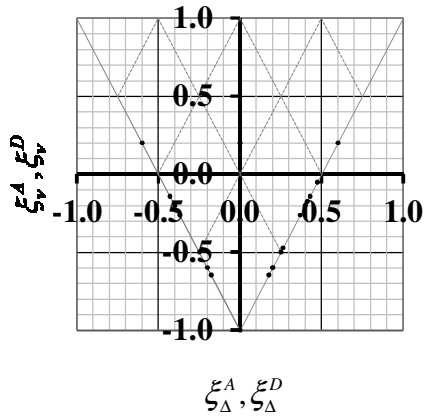
Figure 2.



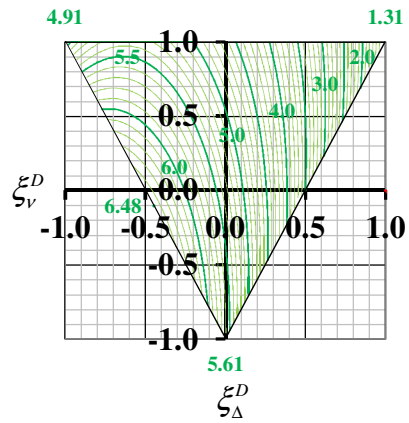
(a)



(d)

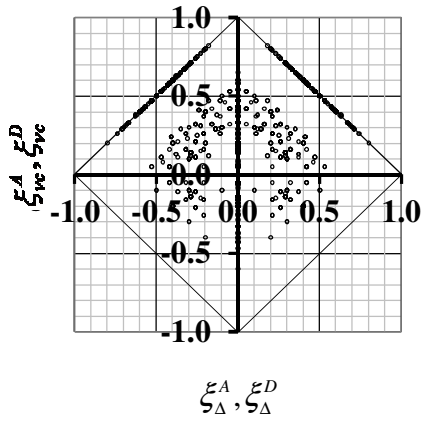


(b)

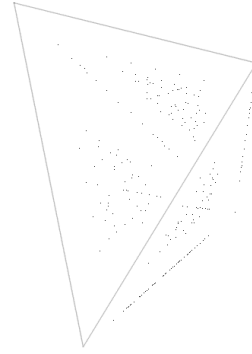


(c)

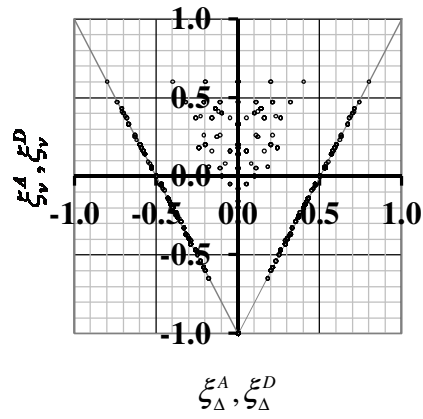
Figure 3



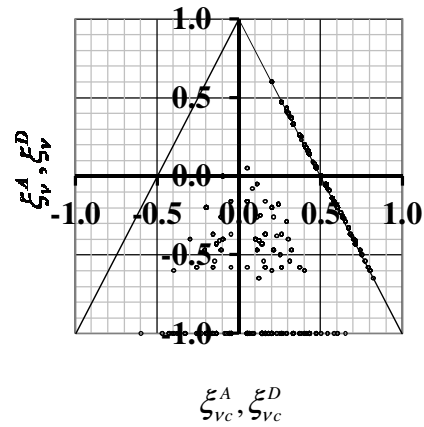
(a)



(d)



(b)



(c)

Figure 4

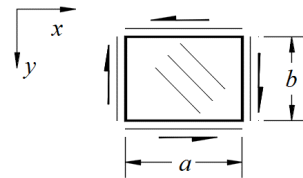
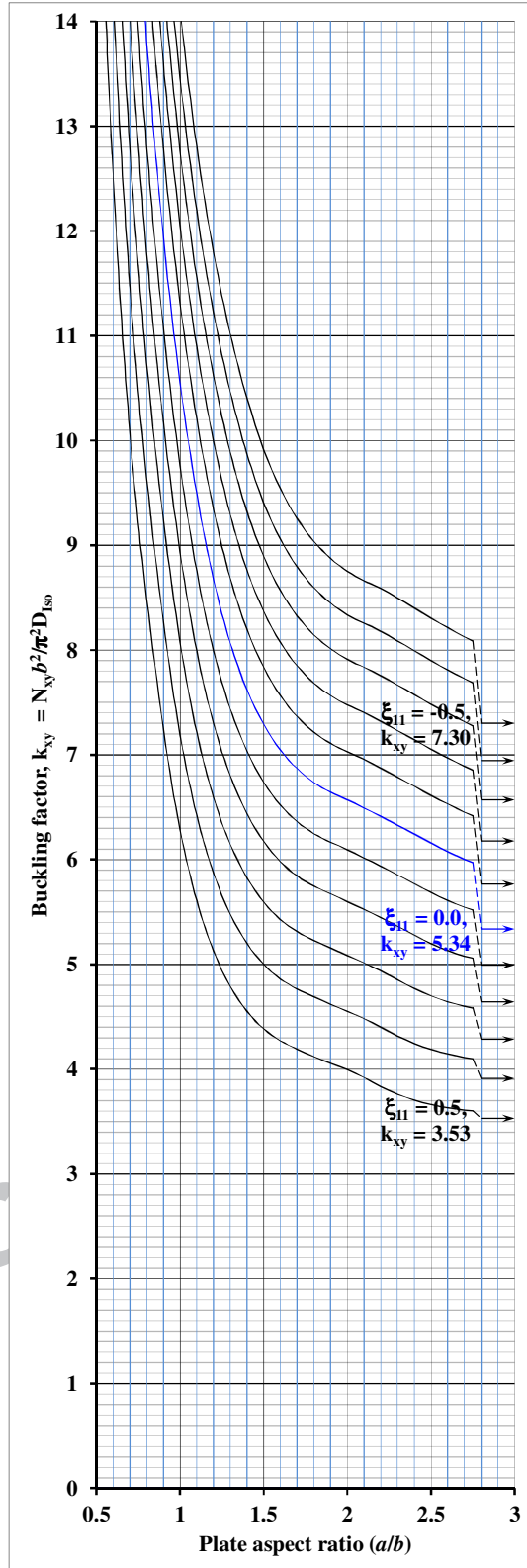


Figure 5(a)

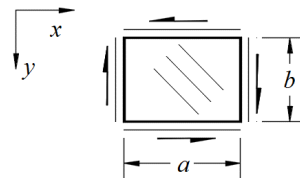
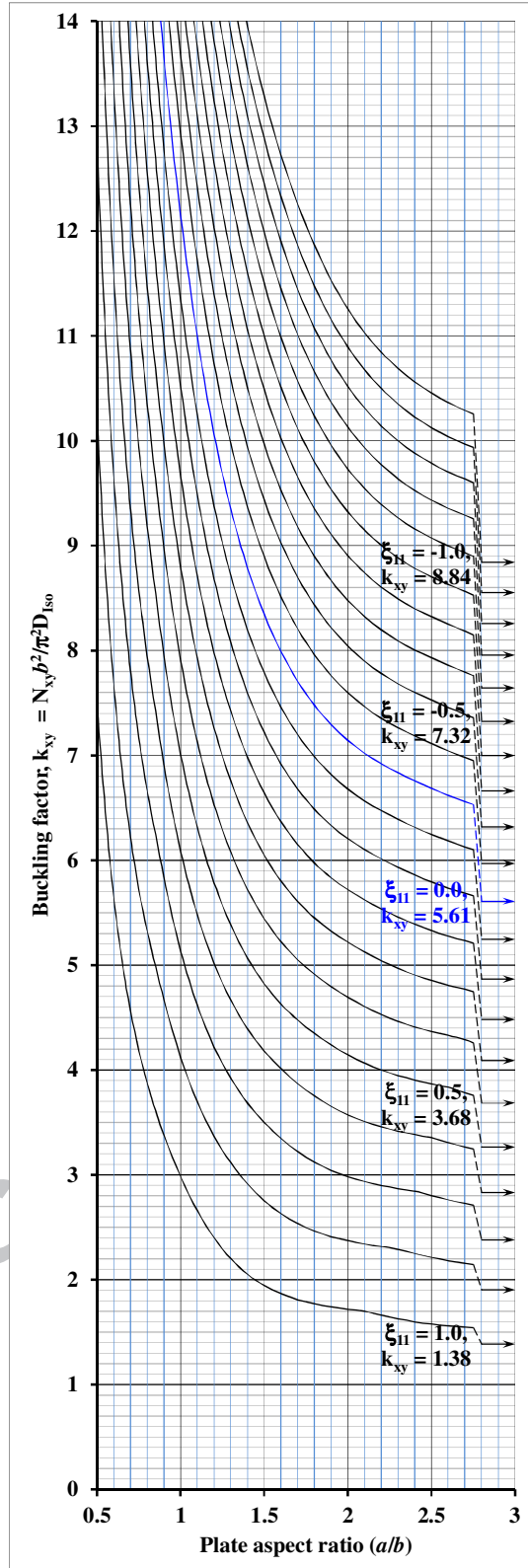


Figure 5(b)

Figure Captions

Figure 1 – Lamination parameter design spaces for the *Extension-Shearing Bending-Twisting* coupled laminates with $7 \leq n \leq 18$, listed in abridged form in Table A6, with Non-symmetric angle-ply and Non-symmetric cross-ply sub-sequences (NN), corresponding to: (a) plan, (b) front elevation and (c) side elevation for extensional stiffness $(\xi_{\Delta}^A, \xi_v^A, \xi_{\Delta c}^A)$ and; (d) plan, (e) front elevation and (f) side elevation for bending stiffness $(\xi_{\Delta}^D, \xi_v^D, \xi_{\Delta c}^D)$.

Figure 2 – Lamination parameter design spaces for the *Extension-Shearing Bending-Twisting* coupled laminates with $3 \leq n \leq 18$, listed in abridged form in Table A10, with Symmetric angle-ply and Symmetric cross-ply sub-sequences (SS), corresponding to: (a) plan, (b) front elevation and (c) side elevation for extensional stiffness $(\xi_{\Delta}^A, \xi_v^A, \xi_{\Delta c}^A)$ and; (d) plan, (e) front elevation and (f) side elevation for bending stiffness $(\xi_{\Delta}^D, \xi_v^D, \xi_{\Delta c}^D)$.

Figure 3 – Lamination parameter design space for: (a) ply percentages, indicating the sub-region used in practical design; (b) Quasi-Homogeneous ($\mathbf{A}_S\mathbf{B}_0\mathbf{D}_S$) laminates, i.e., $\xi_{\Delta}^A = \xi_{\Delta}^D$ and $\xi_v^A = \xi_v^D$, corresponding to the sequence configurations listed in Ref. [1] with $8 \leq n \leq 21$ plies, and indicating the 15 grid points used in the derivation of the 4th order polynomial of Eq. (22) used to generate the: (c) shear buckling contours, $k_{xy, \infty}$ for infinitely long plates with simply supported edges and; (d) mapping of relative angle-ply percentages for Quasi-Homogeneous ($\mathbf{A}_F\mathbf{B}_0\mathbf{D}_F$) laminates, i.e., $\xi_{\Delta c}^A = \xi_{\Delta c}^D$.

Figure 4 – Quasi-Homogeneous ($\mathbf{A}_F\mathbf{B}_0\mathbf{D}_F$) laminate design space, i.e., $\xi_{\Delta}^A = \xi_{\Delta}^D$, $\xi_v^A = \xi_v^D$ and $\xi_{\Delta c}^A = \xi_{\Delta c}^D$, for laminates with $4, 8, 11 \leq n \leq 21$ plies, corresponding to third

angle orthographic projection of: (a) plan view; (b) front elevation and; (c) side elevation for bending stiffness. The Isometric view in (d) is shown to aid interpretation of the point cloud data.

Figure 5 – Shear buckling factor curves for continuous plates with: (a) Quasi-Isotropic laminates $(\xi_{\Delta}^D, \xi_{\nu}^D) = (0, 0)$ and $\xi_{\Delta c}^D = 0, 0.1, 0.2, 0.3, 0.4$ and 0.5 and; (b) Angle-ply laminates $(\xi_{\Delta}^D, \xi_{\nu}^D) = (0, -1)$ and $\xi_{\Delta c}^D = 0, 0.1, \dots, 0.9$ and 1.0 .

ACCEPTED MANUSCRIPT

Tables

Table 1 – Unrestrained thermal (contraction) response of square, initially flat, composite laminates. Stacking sequence configurations containing cross- and angle-ply sub-sequences are representative of the minimum ply number grouping of each class of laminate.

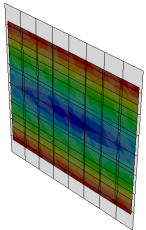
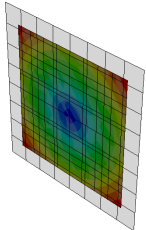
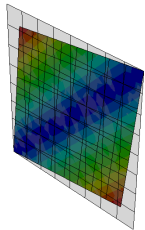
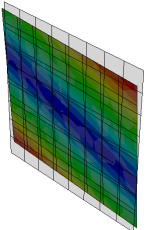
| Uncoupled in Extension (A_S) | | Extension-Shearing (A_F) | |
|--|--|--|--|
| Uncoupled in Bending (D_S) | Bending-Twisting (D_F) | Bending-Twisting (D_F) | Uncoupled in Bending (D_S) |
| $A_S B_0 D_S$ [+/-2/O/+2/-]T | $A_S B_0 D_F$ [+/-/-/+]T | $A_F B_0 D_F$ [+/>+]T | $A_F B_0 D_S$ [±/O/-/O/-3/O/-3/O/+]T |
|  |  |  |  |
| <i>Simple laminate</i> | <i><u>B-T</u></i> | <i><u>E-S;B-T</u></i> | <i><u>E-S</u></i> |

Table 2 – Calculation procedure for the non-dimensional parameters for an $A_F B_0 D_F$ laminate.

| Ply θ | $(z_k - z_{k-1})$ | A | | | | $(z_k^2 - z_{k-1}^2)$ | B | | | | $(z_k^3 - z_{k-1}^3)$ | D | | | |
|--------------|-------------------|--------------|--------------|--------------|-------------------|-----------------------|--------------|--------------|--------------|-------------------|-----------------------|--------------|--------------|--------------|-------------------|
| | | Σ_+^A | Σ_-^A | Σ_o^A | $\Sigma\bullet^A$ | | Σ_+^B | Σ_-^B | Σ_o^B | $\Sigma\bullet^B$ | | Σ_+^D | Σ_-^D | Σ_o^D | $\Sigma\bullet^D$ |
| | | <u>8</u> | <u>0</u> | <u>4</u> | <u>4</u> | | <u>0</u> | <u>0</u> | <u>0</u> | <u>0</u> | | <u>512</u> | <u>0</u> | <u>256</u> | <u>256</u> |
| 1 | + | 1 | → 1 | | | -15 | → -15 | | | | | 169 | → 169 | | |
| 2 | ○ | 1 | | → 1 | | -13 | | → -13 | | | | 127 | | → 127 | |
| 3 | ● | 1 | | | → 1 | -11 | | | → -11 | | | 91 | | | → 91 |
| 4 | + | 1 | → 1 | | | -9 | → -9 | | | | | 61 | → 61 | | |
| 5 | ● | 1 | | | → 1 | -7 | | | → -7 | | | 37 | | | → 37 |
| 6 | + | 1 | → 1 | | | -5 | → -5 | | | | | 19 | → 19 | | |
| 7 | + | 1 | → 1 | | | -3 | → -3 | | | | | 7 | → 7 | | |
| 8 | ○ | 1 | | → 1 | | -1 | | → -1 | | | | 1 | | → 1 | |
| 9 | ○ | 1 | | → 1 | | 1 | | → 1 | | | | 1 | | → 1 | |
| 10 | + | 1 | → 1 | | | 3 | → 3 | | | | | 7 | → 7 | | |
| 11 | + | 1 | → 1 | | | 5 | → 5 | | | | | 19 | → 19 | | |
| 12 | ● | 1 | | | → 1 | 7 | | | → 7 | | | 37 | | | → 37 |
| 13 | + | 1 | → 1 | | | 9 | → 9 | | | | | 61 | → 61 | | |
| 14 | ● | 1 | | | → 1 | 11 | | | → 11 | | | 91 | | | → 91 |
| 15 | ○ | 1 | | → 1 | | 13 | | → 13 | | | | 127 | | → 127 | |
| 16 | + | 1 | → 1 | | | 15 | → 15 | | | | | 169 | → 169 | | |

Table 3 – *Extension-Shearing Bending-Twisting* coupled laminate design space (%) occupied by the various forms of sub-sequence symmetries, including total number (Σ) of configurations, for each ply number grouping. Details for ply groupings for $n = 19$ ($\Sigma = 5,733,946$), 20 ($\Sigma = 2,584,228$) and 21 ($\Sigma = 5,372,297,583$) are not presented, but contain 4.2% (239,263), 8.5% (218,385) and less than 0.1% (961,059) symmetric sequences, respectively.

| n | 7 | 8 | 9 | 10 | 11 | 12 | 13 | 14 | 15 | 16 | 17 | 18 |
|----------|------|------|------|------|-------|-------|--------|-------|--------|--------|---------|---------|
| AC | | | | | | | | | <0.1 | | <0.1 | |
| AN | | | | | | | | | <0.1 | | <0.1 | |
| AS | 3.1 | | 1.9 | | 1.3 | | 0.7 | | 0.3 | | 0.2 | |
| NC | | | | | | | | | 0.1 | | 0.1 | 0.1 |
| NV | 12.3 | 4.0 | 20.6 | 13.4 | 37.3 | 23.5 | 53.1 | 40.1 | 67.9 | 56.2 | 79.5 | 70.9 |
| NS | | | 5.0 | 3.3 | 9.3 | 6.2 | 10.1 | 8.5 | 9.5 | 9.4 | 7.4 | 8.3 |
| SC | | | | | | 0.7 | 1.4 | 1.1 | 0.7 | 0.4 | 0.4 | 0.4 |
| SN | | | 2.5 | | 1.8 | 1.3 | 3.2 | 2.1 | 3.7 | 3.5 | 3.4 | 3.5 |
| SS | 84.6 | 96.0 | 70.1 | 83.3 | 50.3 | 68.3 | 31.5 | 48.2 | 17.7 | 30.5 | 9.1 | 16.9 |
| Σ | 65 | 50 | 321 | 239 | 1,811 | 1,191 | 11,651 | 6,847 | 83,573 | 43,830 | 654,803 | 319,501 |

A – Anti-symmetric; C – Cross-symmetric; N – Non-symmetric; S – Symmetric

AC: [+ / O / ● / - / - / ● / O / - / ● / O / + / + / O / ● / -]_T

NC: [+ / ● / + / O / + / O / + / + / + / ● / + / ● / + / O / +]_T

SC: [+ / ● / O / O / ● / O / ● / ● / O / +]_T

AN: [+ / O / ● / - / - / ● / ● / - / O / ● / + / + / O / ● / -]_T

NN: [+ / ● / ● / ● / + / + / ●]_T

SN: [+ / ● / O / O / ● / ● / ● / O / +]_T

AS: [+ / - / - / - / + / + / -]_T

NS: [+ / - / - / - / ● / + / - / + / -]_T

SS: [+ / - / +]_T

Table 4 – Design space occupied by Quasi-Homogeneous laminates for $11 \leq n \leq 21$ ply *Extension-Shearing, Bending-Twisting* coupled ($\mathbf{A}_F\mathbf{B}_0\mathbf{D}_F$) laminates corresponding to the various forms of sub-sequence symmetries, including total number (Σ) of configurations, for each ply number grouping. The three symmetric 7-ply laminates: $[+/\textcirclearrowleft/+/\textcirclearrowright/+/\textcirclearrowleft/+]$ _T, $[+/-/+/\textcirclearrowleft/+/-/+]$ _T and $[+/\bullet/+/\textcirclearrowleft/+/\bullet/+]$ _T, and the two non-symmetric 8-ply laminates: $[+/\textcirclearrowleft/\textcirclearrowright/+/\textcirclearrowleft/+/\textcirclearrowright/+/\textcirclearrowleft/+]$ _T and $[+/\bullet/\bullet/+/\bullet/\bullet/+/\bullet/\bullet/+]$ _T, are not included.

| n | 11 | 12 | 13 | 14 | 15 | 16 | 17 | 18 | 19 | 20 | 21 |
|----------|----|----|----|----|----|----|-----|----|-----|-----|-----|
| NV | 4 | 2 | 36 | 8 | 32 | 28 | 146 | 56 | 454 | 294 | 254 |
| NS | 2 | - | 10 | 2 | 10 | 4 | 54 | 20 | 124 | 64 | 92 |
| SC | - | - | 2 | - | 2 | - | 2 | 2 | 4 | 2 | 4 |
| SN | - | - | - | - | - | - | - | - | - | - | 4 |
| SS | 6 | - | 3 | 18 | 3 | 14 | 6 | 3 | 15 | 6 | 26 |
| Σ | 12 | 2 | 51 | 28 | 47 | 46 | 208 | 81 | 597 | 366 | 380 |

Table 5 – Transformed reduced stiffness, Q'_{ij} (N/mm²), for IM7/8552 carbon-fiber/epoxy with $\theta = -45^\circ, 45^\circ, 0^\circ$ and 90° .

| θ | Q'_{11} | Q'_{12} | Q'_{16} | Q'_{22} | Q'_{26} | Q'_{66} |
|----------|-----------|-----------|-----------|-----------|-----------|-----------|
| -45 | 50,894 | 40,554 | -37,791 | 50,894 | -37,791 | 41,355 |
| 45 | 50,894 | 40,554 | 37,791 | 50,894 | 37,791 | 41,355 |
| 0 | 162,660 | 4,369 | 0 | 11,497 | 0 | 5,170 |
| 90 | 11,497 | 4,369 | 0 | 162,660 | 0 | 5,170 |

ACCEPTED MANUSCRIPT

Electronic Appendix

The electronic appendix to the main article is provided in a separate document.

ACCEPTED MANUSCRIPT